SSCL-N-870
SSC Cryo Note No. 93-23

Operation and Control of the Helium Cooled Power Leads for the Superconducting Super Collider

J. Demko and V. Datskov

Superconducting Super Collider Laboratory*
2550 Beckleymeade Ave.
Dallas, TX 75237

July 1994

*Operated by the Universities Research Association, Inc., for the U.S. Department of Energy under Contract No. DE-AC35-89ER40486.

OPERATION AND CONTROL OF THE HELIUM COOLED POWER LEADS FOR THE SUPERCONDUCTING SUPER COLLIDER

J. A. Demko and V. I Datskov

SUPERCONDUCTING SUPER COLLIDER LABORATORY[1]
ASD/CRYOGENICS
2550 BECKLEYMEADE AVE, MS4003
DALLAS, TEXAS 75237-3946

OCTOBER 1993

---

1. The SSC Laboratory is operated by Universities Research Association Inc. for the U. S. Department of Energy under Contract No. DE-AC35-89ER40486

ABSTRACT

In order to support the development of controls for the SSC 6.6 kA current leads a review of current lead performance from other designs and a series of operating conditions for the ASST leads has been analyzed. From these results the flows to required to operate the leads at different operating conditions encountered can be determined. The flows provide the basis for the determination of the required control valve flow coefficients. A detailed numerical thermal model of a 6.6 kA power lead for the Superconducting Super Collider previously developed was used for the analysis. The accelerator systems string test (ASST) lead design is used for the analysis. The cryogenic current lead analysis model program (CCLAMP) uses the numerical method of lines (NUMOL) approach to solve for the transient temperature distributions along the lead. The model was developed to provide a tool for analyzing coolant control strategies as well as an understanding of the behavior of the leads under presumed system transients.

INTRODUCTION

The Superconducting Super Collider (SSC) is a high-energy proton accelerator that is being designed and constructed in Texas, just south of Dallas. When the SSC comes on line in the year 2000, it will be the world's largest scientific instrument, with a main ring 87 km (53 miles) in circumference. The SSC will probe the structure of matter at scales below 10^{-18} m to determine if quarks, of which neutrons and protons are composed, are the ultimate particles of matter. In particular, the SSC will be used to search for the top quark if existing accelerators at Fermilab and CERN are unable to find the top in intervening years, and to investigate other aspects of the structure of matter and the fundamental forces within the context of the Standard Model. Also, the SSC will create conditions which are thought to have existed 10^{-18} seconds after the Big Bang.[1]

The accelerating of protons to the 20 Tev level requires powerful steering magnets to be placed around the main ring. The required 6.6 Tesla field can be practically achieved only through the use of low temperature superconducting magnets which will be cooled to 4 K using supercritical helium (He). Thus, electrical power must be delivered from ambient temperature as received from the local power grid to the magnets operating at 4 K. This requirement is achieved using a power lead which must operate through a temperature drop from ambient to 4K. The design of the SSC power leads can significantly affect their performance and efficiency, and therefore the overall power consumption of the SSC.

The design goals for a current lead to be used in a cryogenic installation such as the SSC are (1) that the top end be maintained warm to prevent frost formation that could cause electrical short circuits and possibly mechanical damage to the lead mountings. (2) The cold end must be maintained sufficiently below the transition temperature of the superconducting cable connecting to the magnets so that it does not quench. (3) The heat transfer to the end of the lead at liquid helium temperatures must be below specified limit. (4) The helium consumption used to cool the leads must be below specified limit. (5) It is desirable to obtain stable operation of the leads with minimum impact to the cryogenic system. (6) The lead must have sufficient mass to permit short duration excursions from its design operating point without damage to the lead. The 4 K heat leak and helium cooling flow budgets proposed for some of the SSC leads are provided in Table 1.

The leads will have several operating modes including initial cool down, cold with no current, current ramp, current flat top, and current invert. During each of these operating modes the load to the cryogenics system should be as small as practical without compromising safety or damaging the leads. The results presented here provide a basis for determining the best way to control the coolant flow and achieve this objective.

The normal operation and performance optimization of cryogenic current leads has been the subject of many investigations.[2-14] The transient behavior of helium cooled current leads has also been investigated by Jones et. al.[7], Aharonian et. al.[8] and Demko et. al.[9] Jones investigated the response of a lead to a current overload pulse, and determined conditions for which the lead would become thermally unstable. Aharonian investigated a scenario in which the coolant flow is interrupted to the lead, and what time constants are present. Demko predicted the transients temperatures and coolant flow during a 5000 ampere current ramp experiment with reasonable agreement with the measured data. His model contains a 300 mm long low temperature superconductor at the cold end of the lead in which he shows the advancing of the superconducting transition as a function of time. Additionally, he shows that the use of fixed warm end and cold end temperatures as boundary conditions does not agree with actual operating practice of current leads.

Table 1: Proposed heat leak and cooling flow budgets

Type	Budget 4 K Heat Leak (W)	Budget Mass Flow (g/s)
6.6 kA	7.92	0.396
CEPL	1.20	0.060
By-Pass	0.34	0.012

The dynamic model used here is based on Schiesser[2] which uses the numerical method of lines (MOL). The model was developed to provide a tool for analyzing coolant control strategies as well as an understanding of the behavior of the SSC lead designs under presumed system transients.[6,9] Since the SSC leads will be cooled by supercritical helium, the flow of helium is regulated by a control valve. These leads include a superconducting section at the at the cold end to reduce resistive heating, as well as a normal conducting copper section at the top end. The properties of these materials and of the helium are programmed as functions of temperature in the model. Pressure is also included in the calculation of the He properties, although the pressure drop along the lead is not taken into account since it is small and does not effect the helium properties significantly.

POWER LEAD MODEL

The power lead transient thermal analysis was performed by applying an energy balance to the solid conductor and the helium to compute the helium and conductor temperatures as a function of time and position along the lead. The energy balance equations for the solid and the helium are given by the partial differential equations (1) and (2).

$$\frac{\partial}{\partial t}(\rho_c e_c)\,dv = \frac{\partial}{\partial x}(kA\frac{\partial T_c}{\partial x})\,dx + \alpha_{conv} P\,(T_c - T_v)\,dx + Q_j \qquad (1)$$

$$\frac{\partial}{\partial t}(\rho_v e_v)\,dv = \dot{m}\frac{\partial h_v}{\partial s}ds + \alpha_{conv}P\,(T_v - T_c)\,dx \tag{2}$$

In these equations, e_c and e_v represent the internal energy of the conductor and the helium vapor respectively, ρ_c and ρ_v refer to the density of the conductor and helium vapor, h_v is the helium vapor enthalpy, α_{conv} is the convective heat transfer coefficient and P is the convection surface area per unit length of the lead, m is the helium mass flow rate, T_v and T_c are the helium and conductor temperatures respectively. The quantities *dv*, *dx*, and *ds* are the differential conductor volume, differential distance measured along the axis of the lead, and the differential distance measured along the flow path of the helium respectively, for which the energy balance is written. The joule heating is determined from the following relation:

$$Q_j = \frac{\rho_{elec} I^2}{A_{elec}}dx \tag{3}$$

where the quantities ρ_{elec} and A_{elec} refer to the electrical resistivity of the lead, and the cross sectional area for electrical conduction.

The first term of the right hand side of the helium energy equation can be written in terms of x using equation (4) to relate the distance travelled by the flow to the axial location along the lead.

$$dx = (\pi \times Pitch \times D)\,ds \tag{4}$$

The heat transfer coefficient is determined from a Dittus-Boelter relation when the flow is turbulent (Re > 2000) given in Wilson[14] and for laminar flow the Nusselt number based on the aspect ratio of the channel is a constant from Kays[15]. The heat transfer coefficient is given by equations (5) and (6) for these two flow regimes respectively. In the model, the convection area included two sides of the channel and the channel base. The channel sides were assumed to be isothermal in the radial direction.

$$Nu_{turbulent} = \frac{\alpha_{conv} D_{hyd}}{k_v} = 0.0259 Re^{0.8} Pr^{0.4} \left(\frac{T_v}{T_c}\right)^{0.716} \tag{5}$$

$$Nu_{laminar} = \frac{\alpha_{conv} D_{hyd}}{k_v} = 6.6 \tag{6}$$

The mass flowrate of the helium can be determined using a proportional-integral (PI) control algorithm which adjusts the mass flowrate of the helium to maintain the temperature at the top of the lead at a set point. The equation which describes this control action is:

$$\dot{m} = m_{ss} + K_g \times \left((T - T_{set}) + \frac{1}{\tau} \times \int_0^{\tau} (T - T_{set})\,dt\right) \tag{7}$$

The first term represents the proportional controller with a gain of K_g and the second term is the integral action with a time constant τ. This additional ordinary differential equation can be integrated as part of the solution to provide the mass flow at each time step. For the results given here, the controller gain was set to 0.0 and the mass flow through the leads set by the steady state term m_{ss}.

A convective boundary condition is applied at either end of the lead through an overall heat transfer coefficient determined by engineering judgement. For the cold end, the helium sink temperature was assumed to be 4.2 K and in the baseline runs, the overall heat transfer coefficient was taken to be 1.0 W/cm^2/K. The bottom lead temperature is determined by an energy balance. The flow along the nose piece is laminar for most of the budgeted flow range (at the maximum flow of 0.396 g/s the Reynolds number is 2300). This results in a convective heat transfer coefficient of 0.966 W/m^2/K. Once the flow enters the spiral fin region, the flow area is substantially reduced and the Reynolds number becomes very large. The heat transfer coefficient for the finned region becomes 36.6 W/m^2/K. Thus the heat transfer through the nose piece is dominated by conduction.The warm end sink is 300 K with an overall heat transfer coefficient of 2.0 W/cm^2/K.

This formulation can be simplified by realizing that the heat capacity of the helium is very small compared to the solid conductor so the time derivative in the helium equation may be neglected. By applying an upwind finite difference technique to the enthalpy derivative, the helium energy equation becomes an algebraic expression for determining the helium liquid temperature. The resulting algebraic expression for the helium energy balance is given by equation (8). The enthalpy term and the convective heat transfer coefficient may be evaluated using the conductor temperatures at a given time. This equation can then be used to solve for the new values of the helium vapor temperature along the lead since $h_i = h_i(T_v)$. This approximation is acceptable because the thermal capacitance of the helium is very small in comparison to the lead so the helium temperature changes almost instantaneously with a change in the lead temperature. It is also assumed that there is a small difference between the temperature of the lead and the gas.

In event that the temperature of the gas and lead are significantly different, it is necessary to either solve for the helium temperature iteratively, assuming that the thermal capacitance of the helium is small compared to the lead, or solve the full partial differential equation for the instantaneous energy balance for the helium. Both of these approaches were used and showed no appreciable difference for small temperature differences between the helium and the conductor. The computer run time can be significantly longer for these type solutions. The solutions presented here assume the small temperature difference approximation.

$$\dot{m}\left(\frac{h_i - h_{i-1}}{\Delta x}\right) = \alpha_{conv} P \left(T_c - T_v\right)_i \tag{8}$$

The material properties of the conductor were taken for OFHC copper with a RRR=100. The properties of the Nb-Ti superconductor were based on a copper to superconductor ratio of 1.67. The copper properties are determined from NIST report[16], from Collings[17], and Reed and Clark.[18] The resistivity of the copper joints between sections of the lead and the change of resistivity due to annealing was discussed in Datskov et. al.[19] Special consideration is also required for the superconducting section in calculating the composite thermal conductivity and the electrical current flow when the superconducting transition occurs in this region. The thermal

conductivity as a function of temperature was obtained for the Nb-Ti from Collings.[17] A linear interpolation of all the conductor properties is utilized. The thermal conductivity of the composite region was based on a simple area weighted average of the thermal conductivities. When the Nb-Ti cable is in a superconducting state (i.e. $T < T_{crit}$), it is assumed that the electrical resistivity becomes that of the copper stabilizing the superconductor (based on a copper to superconductor ratio of 1.67) and that all of the current flows through the superconducting cable. The critical temperature was taken to be 9 K assuming no magnetic field.[17]

To solve the resulting system of partial differential equations, the numerical method of lines approach was used as discussed in Schiesser.[20] In this method, the first term on the right hand side of the equation (1), which represents the net conduction heat transfer along the lead, was cast into a finite difference form given by equation (9). The temperature dependent thermal conductivities at the *i+1/2* and *i-1/2* locations were computed based on the geometric mean as recommended by Patankar[21] as given by equation (10).

$$\frac{\partial}{\partial x}\left(kA_c\frac{\partial T}{\partial x}\right) = \frac{(kA)_{i+\frac{1}{2}}\left(\frac{T_{i+1}-T_i}{\Delta x}\right) - (kA)_{i-\frac{1}{2}}\left(\frac{T_i-T_{i-1}}{\Delta x}\right)}{\Delta x} \tag{9}$$

$$k_{i+\frac{1}{2}} = \frac{2k_{i+1}k_i}{k_{i+1}+k_i} \tag{10}$$

Upon making the above algebraic substitutions for the spatial derivatives and applying the required boundary and initial conditions, a system of ordinary differential equations in time results. The LSODES integrator was used to solve the resulting system of ordinary differential equations. A total of 51 equally spaced nodes were used in the model. Spatial convergence was checked by comparing solutions for 101 and 51 equally spaced points.

The pressure drop of the helium across the leads was based on a correlation given in Maehata et. al. [11] for the pressure drop in a spiral shaped tube is given by equation (11). The critical Reynolds number may be determined from equation (12). For laminar flow ($Re<Re_{crit}$), equation (13) is used to obtain the friction factor. For turbulent flow ($Re>Re_{crit}$), equation (14) is used to obtain the turbulent friction factor. The predicted pressure drop is expected to be low using these correlations by about 20% based on comparisons performed by Maehata with measurements in the VENUS current lead.

A figure of merit for the operation of the lead is the Carnot power which combines the ideal work required to liquefy the helium used to cool the leads and the ideal refrigeration required to remove the heat transfer to the 4 K helium. The expression for the Carnot power is given by equation (11). In this expression the environment conditions $T_\infty = 300$ K and $P_\infty = 1.01$ Bar, and the inlet conditions $T_{in} = 4.2$ K and $P_{in} = 4.0$ Bars were used to evaluate the required entropies S_∞ and S_{in} and enthalpies h_∞ and h_{in}.

$$\frac{dP}{ds} = \lambda_p \frac{\rho_v G}{2D_{hyd}} \tag{11}$$

$$Re_{crit} = 20000\left(\frac{D_{hyd}}{D_c}\right)^{0.32} \tag{12}$$

$$\lambda_{p,lam}\left(\frac{D_c}{D_{hyd}}\right)^{0.5} = 1376\left(1.56 + \log Re\left(\frac{D_c}{D_{hyd}}\right)^{0.5}\right)^{-5.73} \tag{13}$$

$$\lambda_{p,turb}\left(\frac{D_c}{D_{hyd}}\right)^{0.5} = 0.029 + 0.304\left(Re\left(\frac{D_{hyd}}{D_c}\right)^{2}\right)^{-0.25} \tag{14}$$

$$P_{Carnot} = \dot{m}\left(T_\infty (S_{in} - S_\infty) - (h_{in} - h_\infty)\right) + \left(\frac{T_\infty - T_{in}}{T_{in}}\right) Q_{4K} \tag{15}$$

Additional parameters that may be used to the overall heat transfer performance of a lead are the heat transfer effectiveness, ε, and number of transfer units, NTU[22]. These are defined in this report by equations (12) and (13) given below. The effectiveness relates the actual heat transferred to the helium to the available potential for heat transfer, and the number of transfer units relates to the heat transfer size of the lead.

$$\varepsilon = \frac{h_{v,out} - h_{v,in}}{h_{c,top} - h_{v,in}} \tag{16}$$

$$NTU = \frac{(T_{v,out} - T_{v,in})}{\dot{m}\,(h_{v,out} - h_{v,in})} \int_x^L UA\,dx \tag{17}$$

6.6 kA POWER LEAD DESCRIPTION

In order to provide background into what can be practically achieved, a review of some of the current leads that are available has been performed. Table 2 provides a summary of the operating parameters of current lead designs from several laboratories and institutes. On a per kiloampere basis, all of the leads operate within small flow and heat leak margins of each other. Some measured temperature data is available for a few of the cases in the table. The VENUS lead described by Maehata is similar in construction to the ASST design. For the 10 kA design the top and bottom temperatures were reported to be approximately 232 K and 7 K respectively at the design current for stable operation. The CERN lead was operated using a thermostatic valve to control coolant flow. Values measured for operation with and without the valve are shown in

Table 3. The data indicates that stable operation may be obtained with the top end of the lead warm by proper control of the lead coolant flow.

An isometric view of the ASST lead pair the assembly is shown in Figure 1.This figure illustrates the flange mounting of the leads to the feed and end can vacuum vessels, and the bellows on the end of the leads where they penetrate into the helium flow region. Details of the actual current carrying and heat transfer sections of the lead are provided in Figure 2 which is an assembly drawing of the ASST lead. In Figure 2 it is shown that the lead was fabricated from 5 finned sections and a final nose piece section that were soldered together. The last two sections and the nose piece section contain Nb-Ti superconductor cable. The superconductor is sandwiched between two half-round sections and soldered into the hollow finned sections and nose piece section. The scope of the current model is the finned section between the flag and the nose piece.

The power lead has a core diameter of 1.59 cm. There are approximately 3.15 fins/cm. The fin thickness and spacing are 0.159 cm. The depth of the spiral fins was held constant at 1.18 cm. providing a constant cross sectional area of 0.188 cm^2 for the helium flow. An Nb-Ti superconductor cable surrounded by a copper casing is included in the first 30 cm. of the leads length. The cable has a rectangular cross section given as 0.813 cm. x 0.305 cm. resulting in a cross sectional area for the Nb-Ti of 0.248 cm^2. An assumed copper to superconductor ratio for

Table 2: Comparison of operating parameters for leads

	I (A)	*Q (@ I=0)* (W)	*Q/I* (W/kA)	*m* (g/s)	*m/I* (g/s/kA)	mV	*ΔP* (kPa)
HERA[10]	6500	20.8[a]	3.2+/-.3[a]	0.34	0.052	29.	
MAEHATA[11]	7000	7.47	1.07	0.387	0.055		11.6
(KEK)	10000	10.4	1.04	0.506	0.049		6.87
CERN[12]	1600	2.72	1.7				
LBL	2000	3.0	1.5				
AMI (1.4 lit/h/kA)	6600.			0.321	0.049	110.	0.2
JINR/LHE[13]	4000	4.0 (2.5)	1.0	0.2	0.05		10.
	6000 (6kA)	6.0 (4.0)	1.0	0.3	0.05		12.
	(7kA)	6.72 (3.5)	1.12	0.316	0.053		10.
	(9 kA)	7.02 (6.0)	1.17	0.351	0.059		11.

a. Values shown are for combination of heat leak and boil-off.

the cable of 1.67 was also used in this model. The remainder of the lead core is solid copper. The total length of the lead is 76.64 cm. for the accelerator system string test (ASST) leads and 83.5 cm for prototype leads tested at Fermi National Atomic Laboratory (FNAL) not including the end hardware used to connect to connect to the power supply or to the cryogenic device. The whole lead is convective cooled by liquid helium that enters at 4 K and a pressure of 4 atmospheres. The cooling passages spiral around the outside of the lead removing heat from the lead. Heat transfer

results from two sources that include conduction from the room temperature environment to the cryogenic helium conditions at the cold end, and from internal heat generation from the resistance of the lead to the flow of electrical current.

Table 3: CERN lead top temperature comparison for *different modes of coolant control*

Mode	I (A)	TOP TEMP (K)
Without thermostatic valve	0	220
	1600	270
With thermostatic valve	0	283
	1600	286

COOLDOWN ANALYSIS

Figure 3 is an approximated cool down of the lead. The lead is initially at 300K and the helium flow past the bottom of the lead is 4.2 K. The development of the temperature profiles as a function of time is shown. No helium is allowed to flow through the lead for this phase of the cooldown. The cooldown time to a steady state condition occurs after 2000 seconds (33 minutes). At steady state for no flow through the lead, the top end is at 291 K, the bottom end is at 24 K, and about 39 W of heat transfer occurs to the 4 K. This condition is unacceptable for allowing current to flow to the magnets since the bottom end is above the transition temperature for Nb-Ti.

STEADY STATE RESULTS

Comparisons of predictions with the CCLAMP model and measurements have been documented for a test of prototype lead under steady state[6] and transient[9] operation. The predictions compared favorably with the temperature measurements but there was some disagreement between the predicted and measured voltage drop. In addition, there were no experimental results for the heat leak or off-design transients. Test data for these conditions would be very useful in validating the model.

Comparisons of the feed can lower bus lead top and bottom temperatures and upper bus top temperature data from the ASST run 3 data is shown in Figures 4 through 7 for cases with no current. Figures 4 and 5 show the sensitivity of the calculations to variations in the convective boundary condition coefficient UA(1) which was varied from 0.1 to 1.0. The ASST run 3 bottom temperature data are contained within the envelope resulting from varying UA(1). The lead top temperature predictions change only slightly due to the variation in UA(1).

The effects of varying the top end convective boundary condition coefficient UA(NG) is shown in Figures 6 and 7 for the bottom and top end temperatures. For a range of the coefficient UA(NG)=1.0 to UA(NG)=2.0 there is almost no change in the predicted bottom end temperatures. In Figure 7 the measured top end temperatures all fall between these limits. The baseline values mentioned previously of UA(1)=1.0 and UA(NG)=2.0 reasonably reflect the expected operation of the ASST design 6.6 kA leads for collider operation.

The 4 K heat transfer and Carnot refrigeration load for the no current case is shown in Figures 8 and 9 for the baseline coefficients. The heat transfer continues to decrease as the mass flow increases. The Carnot power has a minimum near 0.2 g/s.

Figures 10, 11 and 12 show the top temperature, bottom temperature, and 4 K heat transfer for cases with currents from 1 to 7.5 kA. For the 5 kA and above cases, the predictions indicate that the leads will not be thermally stable if the mass flows are decreased 0.005 g/s from the lowest value shown. Thus, this may be taken as the thermal limit of the lead. Figure 10 indicates that it is probably not possible under the present assumptions to operate the lead at current without frosting the top. At currents of 5 kA or below, it may be possible to keep the flag warm but at the expense of a high heat transfer to the 4 K as shown in Figure 12 and being close to the superconductor critical temperature as shown in Figure 11. Figure 13 shows the Carnot power required to cool an individual lead for the different currents and mass flows. There is a flow which minimizes the Carnot power for each of the currents shown although at currents greater than 6 kA the minimum occurs near the predicted limit of the leads operation.

The voltage drop across the lead is shown in Figure 14. The voltage drop is monitored by the quench protection system and when it exceeds 30 mV, the power is turned off. This setting is conservative and does not permit optimal operation of the leads at the higher currents.

The helium exit pressure as calculated by the method described in Maehata[11] is shown in Figure 15. These results may under estimate the pressure drop by as much as 22%, but in any case the pressure drop is probably under 10 kPa. For currents between 1000 to 4000 amperes, the pressure drop decreases almost linearly with increasing mass flow. This is because the helium exits the lead at fairly cold temperatures. For currents of 5000 amperes and above, there are relatively high temperatures near the top of the lead which produces lower density flow and higher pressure drops through the lead.

As discussed earlier in this report, there is some concern as to the heat transfer through the bottom of the lead. A study of the sensitivity to this for the design current of 6,600 amperes has been conducted. The results for the affect of the bottom end heat transfer coefficient on the top temperature, bottom temperature and 4 K heat transfer are shown in Figures 16, 17, and 18 for a variation in the heat transfer coefficient from 0.1 to 1.5 $W/cm^2/K$. As was demonstrated previously, this magnitude of variation in the heat transfer coefficient can be realized between laminar and turbulent flow. The top temperature of the lead changed a few degrees K with a 10 times variation of the heat transfer for the lower flow rates. The bottom end temperature changed just under 1 K due to this variation in the heat transfer coefficient. It is therefore important to properly design the low end flow path in order to keep the heat transfer coefficient and surface area as high as is practical.

FLOW COEFFICIENTS

The flow coefficients can be determined directly from the mass flow required to maintain the leads in stable condition. Additional constraints are that the heat leak to the 4 K be under 7.9 W per lead, the mass flow through each lead not exceed 0.396 g/s^1, and the bottom of the lead must be maintained sufficiently below the critical temperature for the Nb-Ti superconductor. Some operating goals are to maintain the top end warm to prevent frost buildup and to minimize the load to the cryogenics plants. The minimum Carnot power values generally meet these criteria, and are selected as the operating points for the different currents as provided in Table 4.

In Table 5 are the operating conditions of the helium at the inlet and outlet of the lead. In addition, a flow coefficient C_v for a control valve downstream of the lead is shown. The value of C_v assumes that the pressure downstream of the valve (i.e. in the lead flow header) is 1.5 bars. No pressure drop for the lines from the discharge of the lead to the control valve are included in this evaluation.

CONCLUSIONS AND RECOMMENDATIONS

Examples of leads used at other major institutions and laboratories as well as their operational characteristics has been summarized. It has been demonstrated that proper lead design and a proper coolant control strategy can be realized which will meet the stated goals for the design and operation of the power leads for the Superconducting Super Collider Laboratory. Leads for the Superconducting Super Collider can be made to meet the heat leak and mass flow budgets as well as operate with a top end temperature above the dew point through a combination of proper mechanical design and coolant flow control. This has been demonstrated at both CERN and JINR.

A method of lines solution procedure has been employed to determine the transient temperature and voltage distributions in a prototype 6500 amp current lead for the Superconducting Super Collider. The predictions are in fair agreement with measured data.

The mass flows used in the operation of the lead can be determined from the minimum Carnot power of the cryogenic system. For the ASST lead design, the lead cannot operate with a warm top, so there will be frost building up whenever the power is on. Some means to prevent frost build up is required in order to prevent electrical shorting and possible mechanical damage to the warm end of the leads for the collider design. Therefore mechanical design changes and/or a control strategy must be implemented that either prevent the warm end from frosting up or to control the frost build up so that electrical shorting and mechanical damage to the leads will not occur. It is important to have test data to assess the empirical model coefficients used in the application of boundary conditions in order to have reliable predictions. This can best be achieved through experimentation with leads at representative operating conditions.

Table 4: Operating parameters for ASST 6.6 kA lead

I (kA)	Mass Flow (g/s)	T_{top}(K)	T_{bot}(K)	Q(W)	Voltage	Carnot Power (W)
0.0	0.200	241.4	5.544	5.0915	0.00000E+00	1778.59
1.0	0.200	242.2	5.578	5.2808	0.49138E-02	1791.92
2.0	0.200	244.8	5.681	5.8935	0.10303E-01	1835.07
3.0	0.225	243.5	5.329	4.2139	0.14869E-01	1894.28
4.0	0.225	251.1	5.587	5.5834	0.22774E-01	1990.73
5.0	0.250	255.5	5.398	4.7417	0.30182E-01	2108.95
6.0	0.285	259.8	5.018	3.1423	0.37515E-01	2244.81
6.6	0.305	266.7	4.874	2.5960	0.44904E-01	2348.33
7.0	0.320	274.4	4.809	2.3683	0.52490E-01	2438.80
7.5	0.345	274.3	4.589	1.5078	0.53914E-01	2555.69

Table 5: Operating parameters for ASST 6.6 kA lead flow

I (kA)	Mass Flow (g/s)	T_{in} (K)	P_{in} (Bar)	T_{out} (K)	P_{out} (Bar)	C_v (g/s/Bar)
0.0	0.200	4.2	4.0	218.5	3.977	0.0807
1.0	0.200	4.2	4.0	219.6	3.977	0.0807
2.0	0.200	4.2	4.0	223.2	3.976	0.0807
3.0	0.225	4.2	4.0	218.6	3.972	0.0910
4.0	0.225	4.2	4.0	229.5	3.969	0.0911
5.0	0.250	4.2	4.0	247.4	3.962	0.1015
6.0	0.285	4.2	4.0	252.1	3.953	0.1162
6.6	0.305	4.2	4.0	259.9	3.944	0.1248
7.0	0.320	4.2	4.0	268.7	3.935	0.1314
7.5	0.345	4.2	4.0	268.4	3.931	0.1420

NOMENCLATURE

A_c - Cross sectional area of the conductor (cm^2).

e_c, e_v - Internal energy of the conductor and the helium vapor respectively, (J/g).

h_∞ - Helium enthalpy at environment temperature and pressure (J/g).

h_{in} – Helium enthalpy at inlet temperature and pressure (J/g).

h_v - Helium vapor enthalpy, *(J/g)*.

i - Finite difference node index.

I - Electrical current (amperes).

k - Thermal conductivity (W/cm/K).

m - is the helium mass flow rate, (g/s).

Nu_{lam} - Laminar flow Nusselt number.

Nu_{turb} - Turbulent flow Nusselt number.

P - Convection surface area per unit length of the lead, (cm^2/cm).

Pr - Prandtl number of the helium.

P_{Carnot} - Cryogenic system Carnot power (W).

P_{in} - Helium inlet pressure set to 4.0 Bars.

P_∞ - Environment pressure set to 1.01 Bar.

Q_j - Joule heating (W)

Q_{4K} - Heat transfer to the 4 K (W)

Re - Reynolds number of the helium flow.

S_∞ - Helium entropy at environment temperature and pressure (J/G/K).

S_{in} - Helium entropy at inlet temperature and pressure (J/g/K).

T_v, T_c - The helium and conductor temperatures respectively (K).

T_{bot} - Lead conductor temperature at bottom end of lead (K).

T_{top} - Lead conductor temperature at top end of lead (K).

T_∞ – Environment temperature set to 300 K.

T_{in} – Helium inlet temperature set to 4.2 K.

x - Distance along the axis of the lead (cm).

dv - Differential conductor volume, (cm^3).

dx - Differential distance measured along the axis of the lead, (cm).

ds - Differential distance measured along the flow path of the helium, (cm).

α_{conv} - Convective heat transfer coefficient

ρ_c, ρ_v - Density of the conductor and helium vapor, (g/cm^3).

ρ_{elec} - Electrical resistivity of the material (Ohm-cm).

REFERENCES

1. J. R. Sandford and D. M. Matthews," Site-Specific Conceptual Design of the Superconducting Super Collider", SSCL-SR-1056, July 1990
2. W. E. Schiesser, "A Dynamic Model of the SSC Power Leads", SSC Laboratory Informal Report, August 1990
3. R. McFee,"Optimum Input Leads for Cryogenic Apparatus", The Review of Scientific Instruments, Volume 30, Number 2, February 1959
4. Yu. L. Buyanov, "Current Leads for Use in Cryogenic Devices. Principle of Design and Formulae for Design Calculations", Cryogenics, Vol. 25, February 1985
5. M. Maehata, K. Ishibashi, M. Wake, A. Katase, and M. Kobayashi,"Optimization Method for Superconducting Magnet Current Leads", Cryogenics, Vol. 28, November 1988
6. J. A. Demko, W. E. Schiesser, R. Carcagno, M. McAshan, and R. McConeghy, R.,"Thermal Optimization of the Helium Cooled Power Leads for the SSC", Presented at the IISSC, New Orleans, La., March 1992
7. M. C. Jones, V. M. Yeroshenko, A. Starostin, and L. A. Yaskin,"Transient Behavior of Helium-Cooled Current Leads for Superconducting Power Transmission", Cryogenics, June 1978
8. G. Aharonian, L. G. Hyman, and L. Roberts,"Behavior of Power Leads for Superconducting Magnets", Cryogenics, March 1989
9. J. A. Demko, W. E. Schiesser, R. Carcagno, and M. McAshan, "A Method of Lines Solution of the Transient Behavior of the Helium Cooled Power Leads for the SSC", Proceedings of the 7th Annual IMACS Conference on the Solution of Partial Differential Equations, Rutgers University, June 1992
10. I. Ben-Zvi, B. V. Elkonin, J. S. Sokolowski, and D. Sellmann, "Current Leads for HERA," Nuclear Instruments and Methods in Physics Research, A276, 1989
11. K. Maehata, S. Kawasaki, K. Ishibashi, Y. Wakuta, H. Kawamata, and T. Shintomi, "Operational Performance of Spiral Fin Current Leads," Cryogenics, Vol. 33, No. 7, 1993
12. H. Blessing and Ph. Lebrun, "Development of Modular Thermostatic Vapor-cooled Current Leads for Cryogenic Service," CERN Report 83-11, November 1983.
13. V. D. Bartenev and Yu. A. Shishov, "Force-cooled Current Leads for the Force-cooled Superconducting Magnets of the Nuclotron," Cryogenics, Vol. 31, November 1991.
14. M. N. Wilson, Superconducting Magnets, Clarendon Press, Oxford, 1982
15. W. Kays, "Convective Heat and Mass Transfer", McGraw-Hill, 1966
16. N. J. Simon, E. S. Drexler and R. P. Reed, "Properties of Copper and Copper Alloys at Cryogenic Temperatures", NIST Monograph 177, February 1992
17. E. W. Collings, "Applied Superconductivity, Metallurgy, and Physics of Titanium Alloys", Plenum Press, 1986
18. R. P. Reed and A. F. Clark, "Materials at Low Temperatures", American Society for Metals, 1983.
19. V. I. Datskov, J. A. Demko, S. D. Augustynowicz, and R. Hutton, "An Experimental Evaluation of Joint Electrical Resistance on Power Lead Thermal Performance", Proceedings of the Fifth Annual International Industrial Symposium on the Super Collider, May 6-8, 1993, San Francisco, Ca., Plenum Press, Also as SSCL-Preprint-203.

20. W. E. Schiesser, "The Numerical Method of Lines Integration of Partial Differential Equations", Academic Press, San Diego, 1991

21. S. V. Patankar., "Numerical Heat Transfer and Fluid Flow", Hemisphere Publishing Corporation, 1980

22. W. Kays and A. L. London, "Compact Heat Exchangers", McGraw-Hill Inc., 1964.

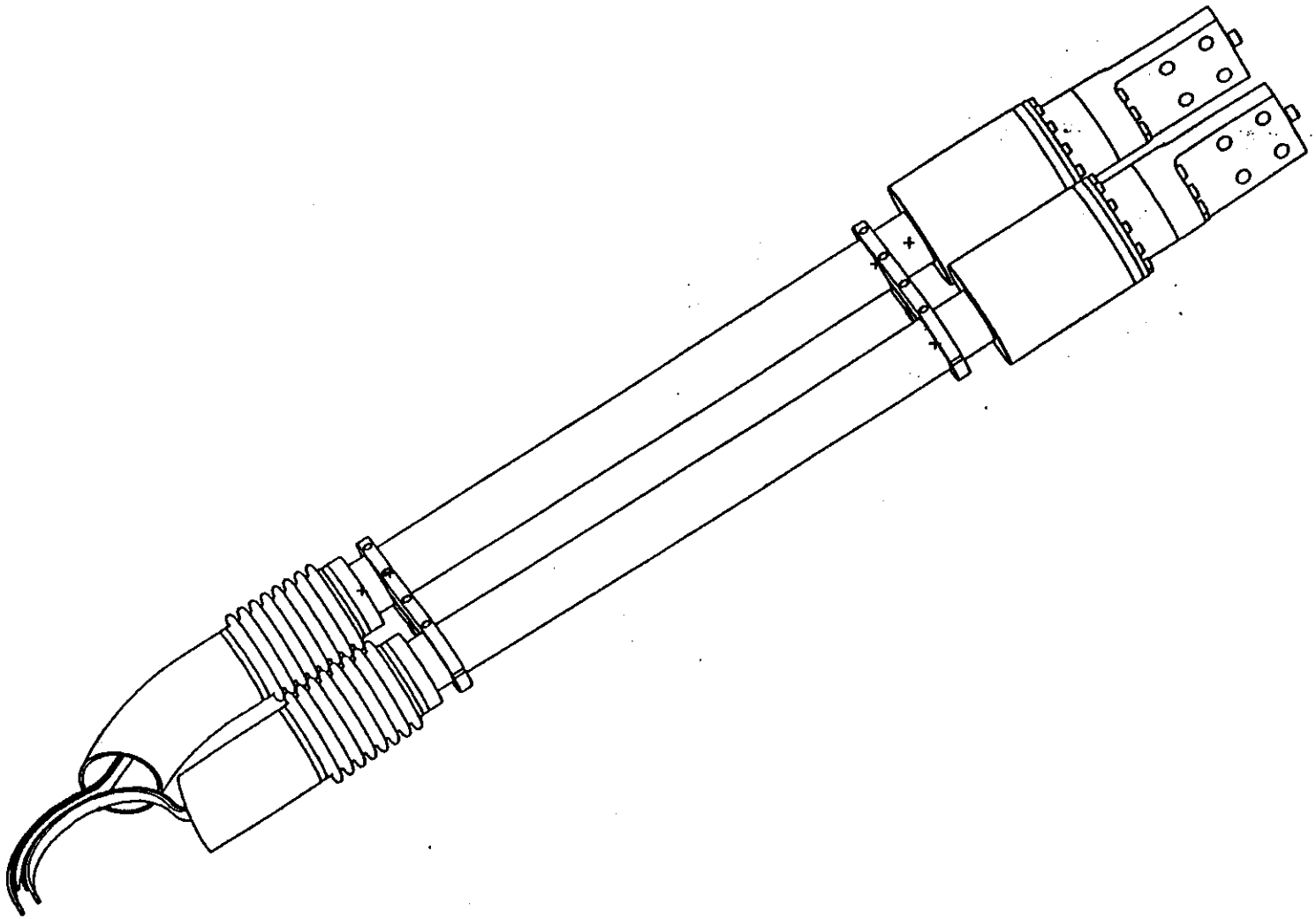

FIGURE 1: ISOMETRIC VIEW OF THE ACCELERATOR SYSTEMS STRING TEST (ASST) LEAD PAIR

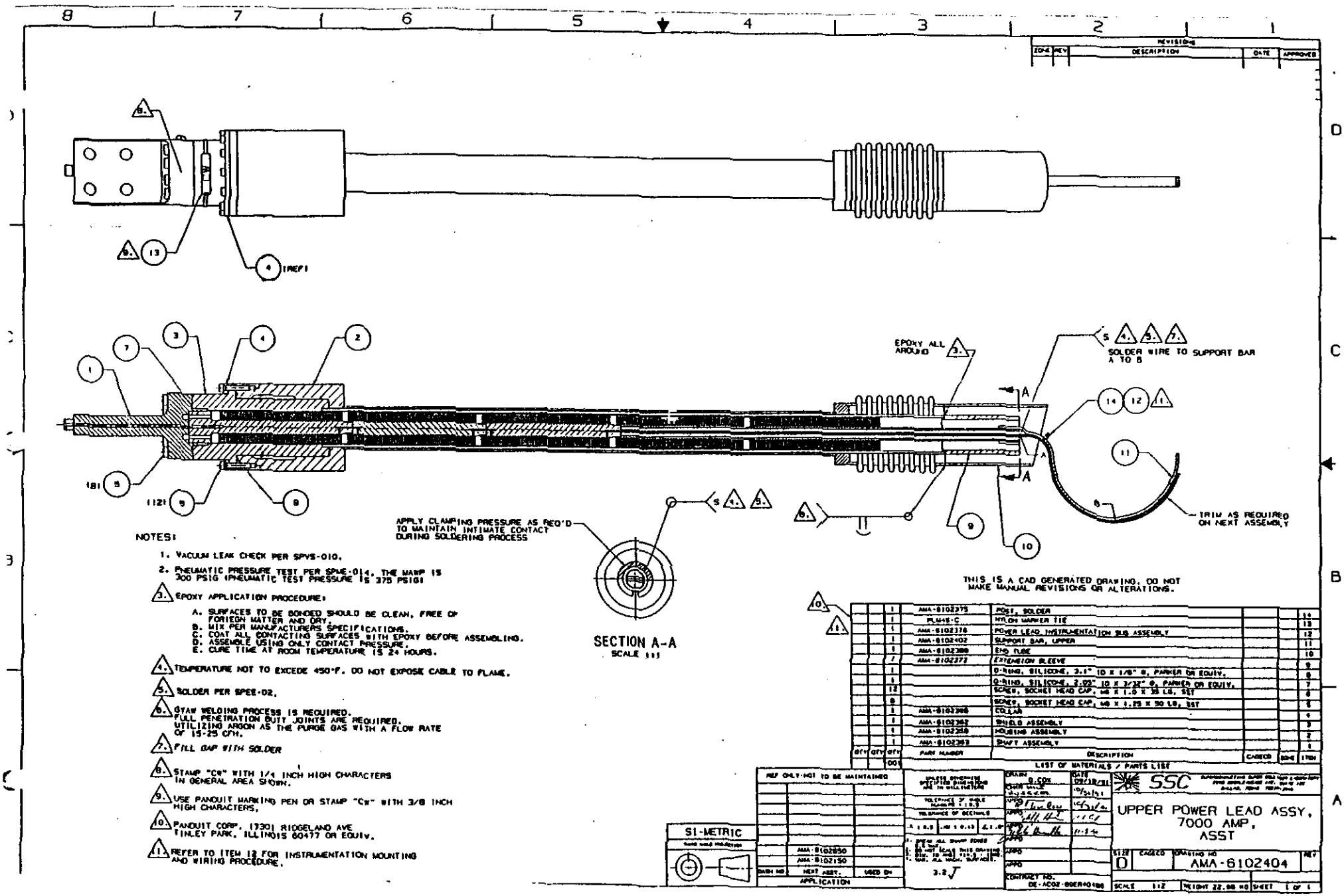

FIGURE 2: ASST 7000 AMPERE POWER LEAD ASSEMBLY DRAWING

FIGURE 3: ASST LEAD INITIAL COOLDOWN ANALYSIS
TRANSIENT TEMPERATURE DISTRIBUTIONS
HEAT TRANSFER AT LEAD BASE ONLY

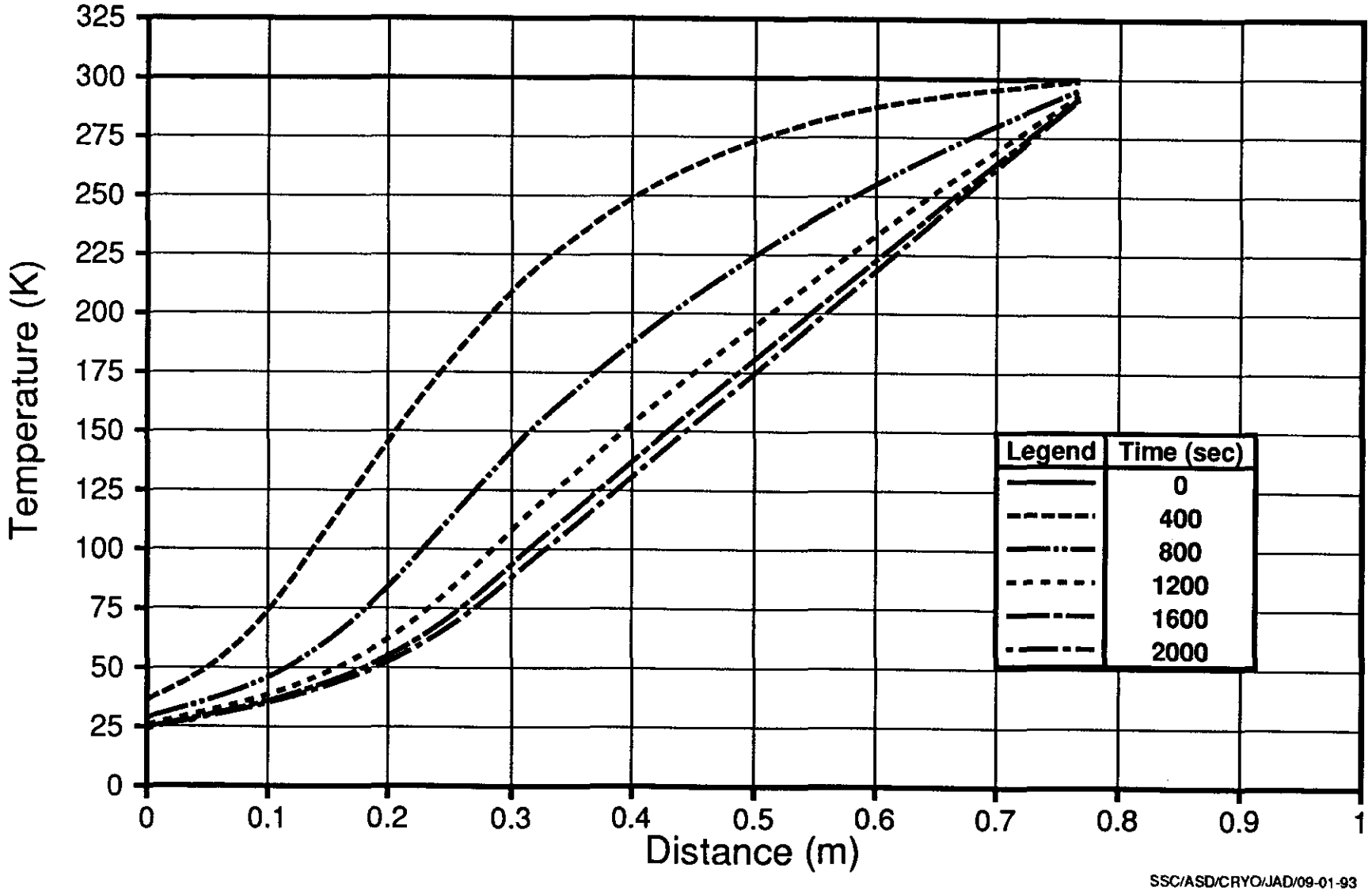

SSC/ASD/CRYO/JAD/09-01-93

FIGURE 4: ASST LEAD COLD END TEMPERATURES FOR STEADY STATE AT I=0 KA

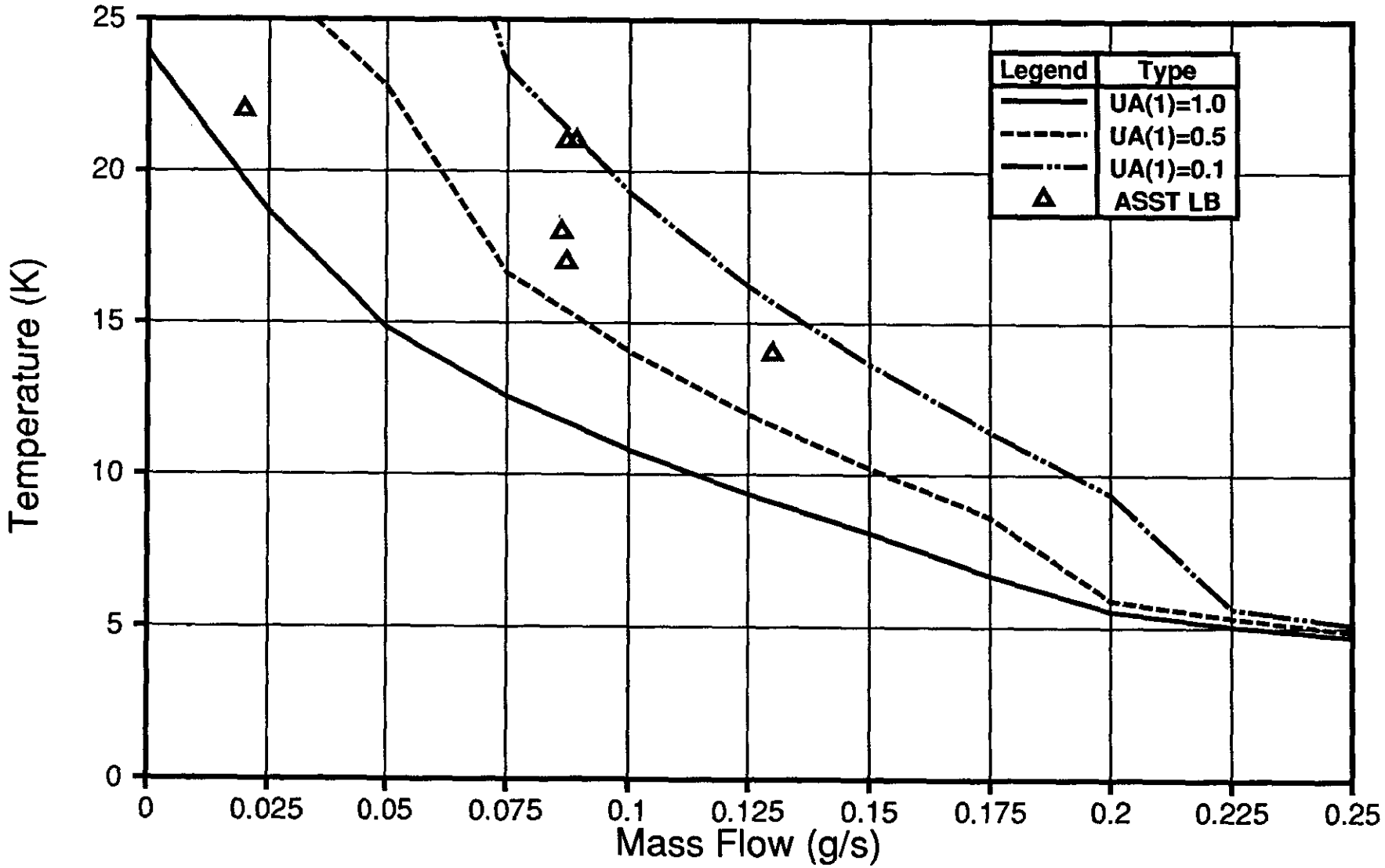

SSC/ASD/CRYO/JAD/04-OCT-93

FIGURE 5: ASST LEAD WARM END TEMPERATURES FOR STEADY STATE AT I=0 KA

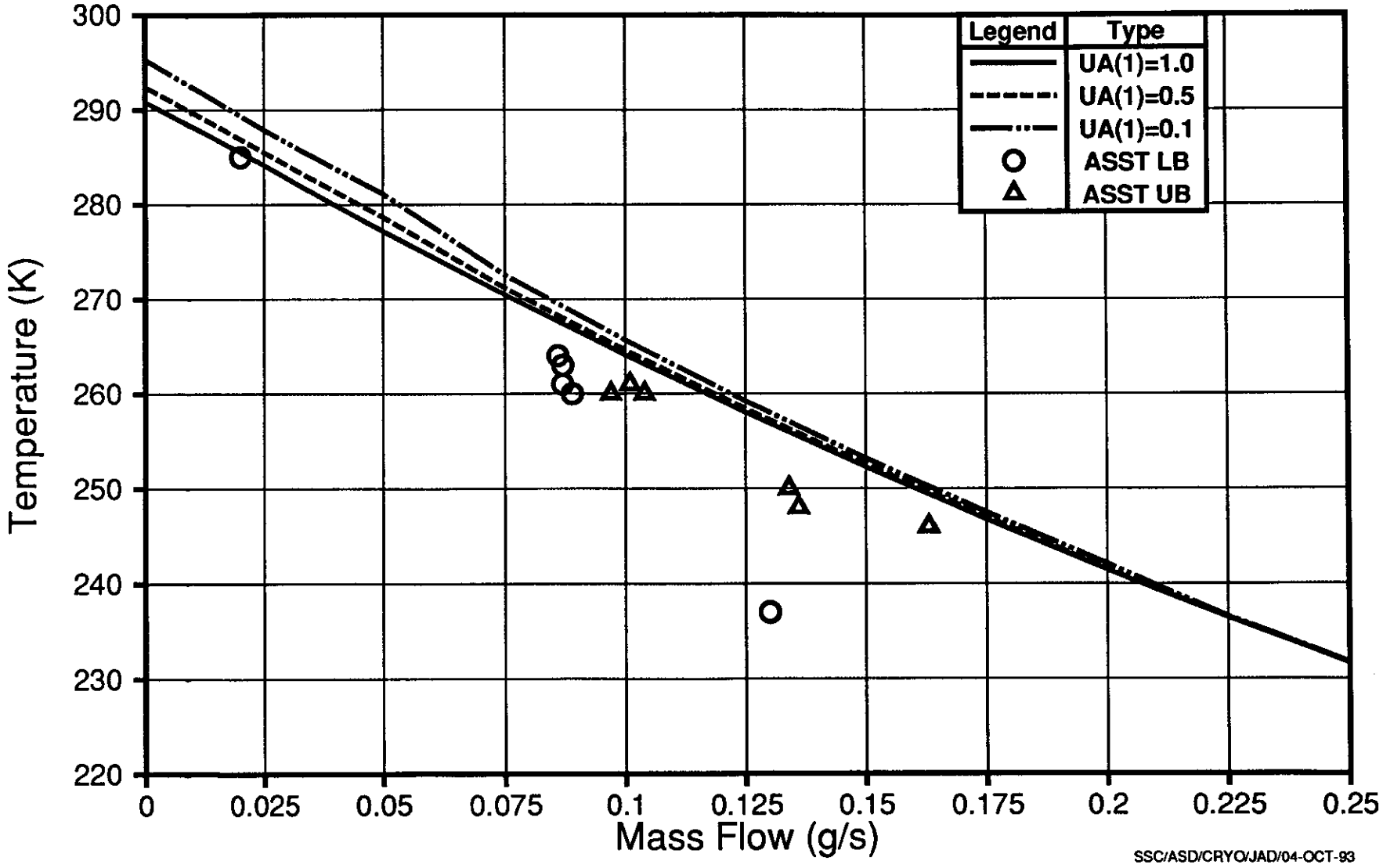

FIGURE 6: ASST LEAD COLD END TEMPERATURES FOR STEADY STATE AT I=0 KA

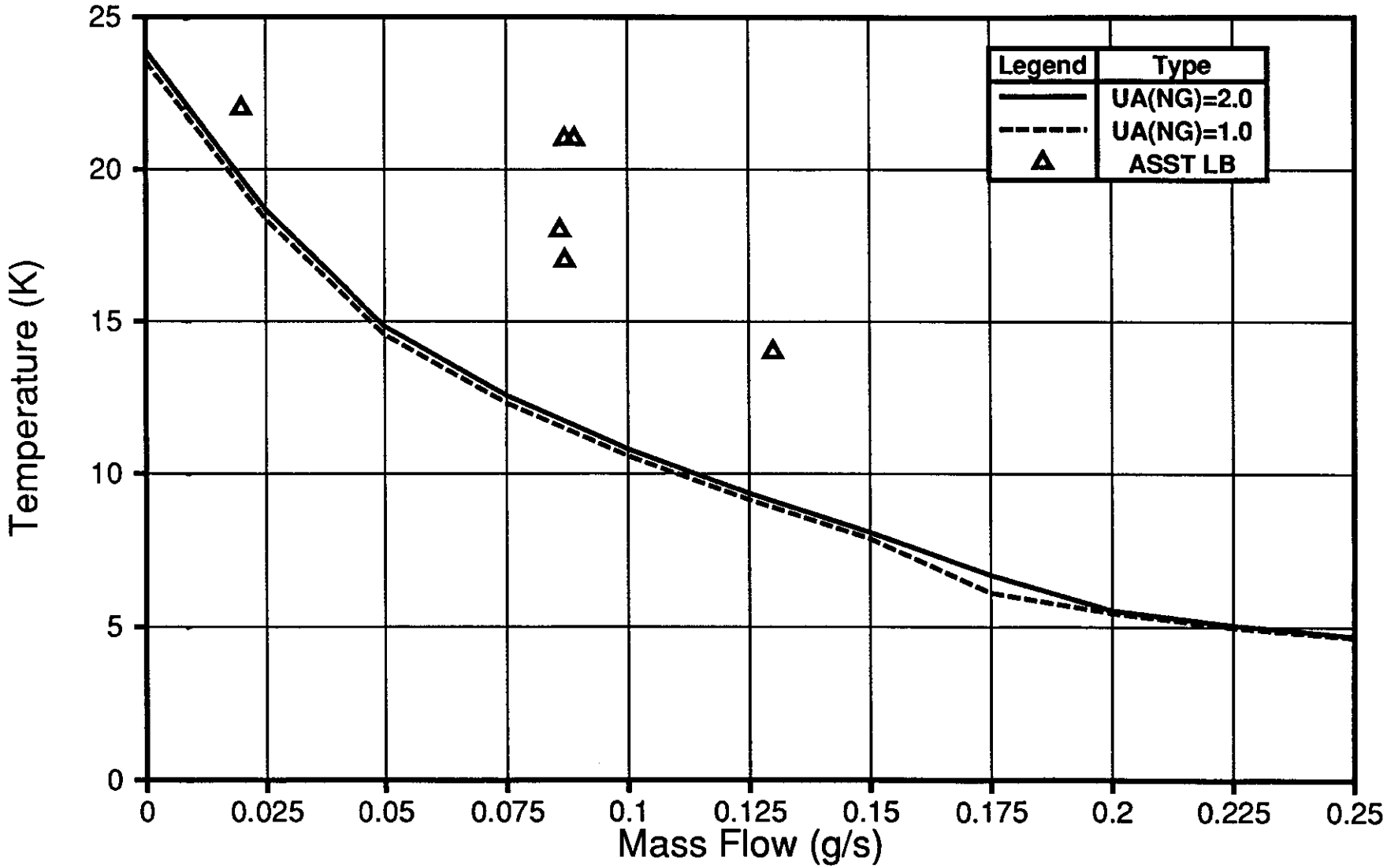

SSC/ASD/CRYO/JAD/04-OCT-93

FIGURE 7: ASST LEAD WARM END TEMPERATURES FOR STEADY STATE AT I=0 KA

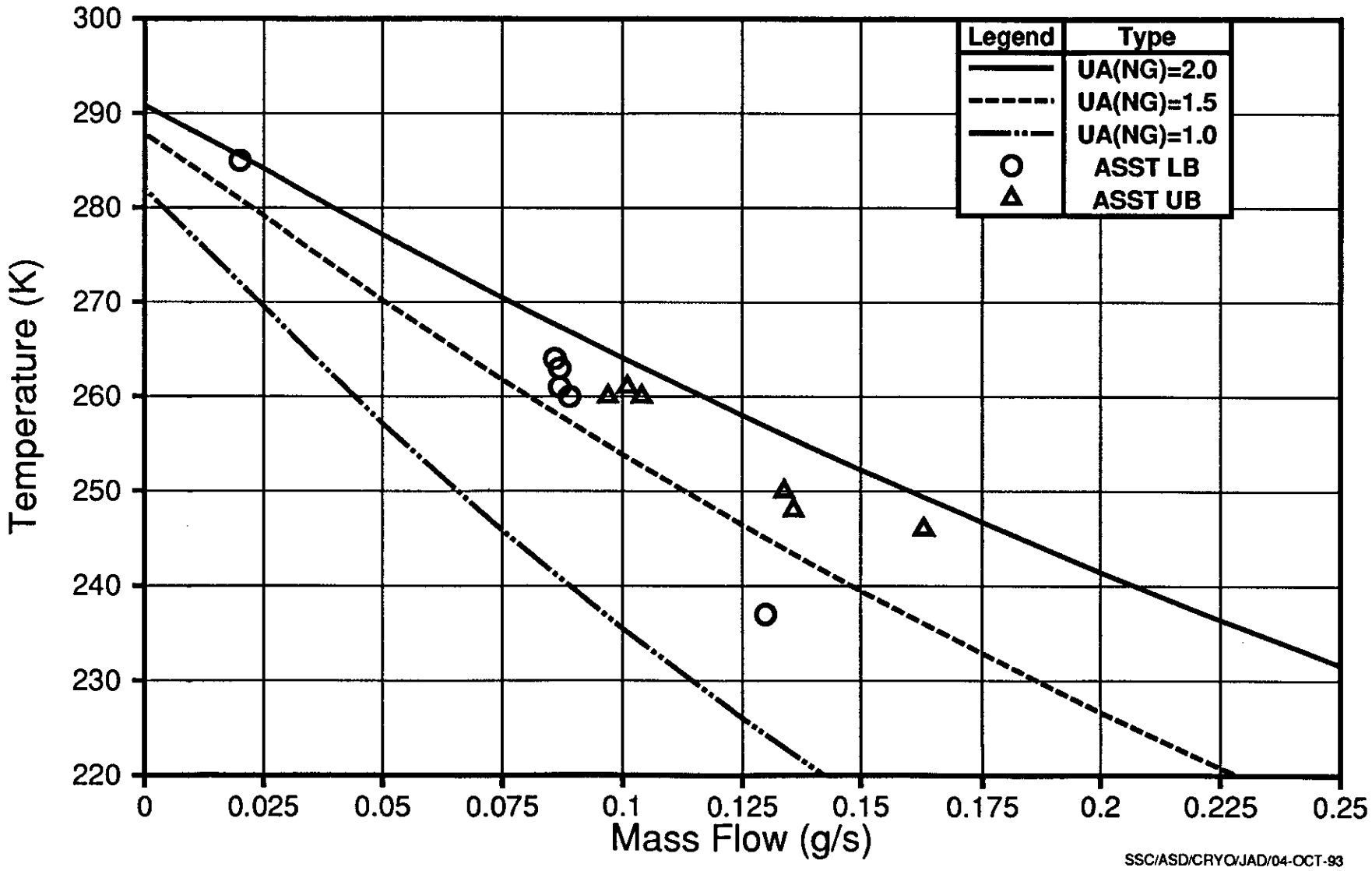

FIGURE 8: ASST LEAD 4 K HEAT TRANSFER FOR STEADY STATE AT I=0 KA

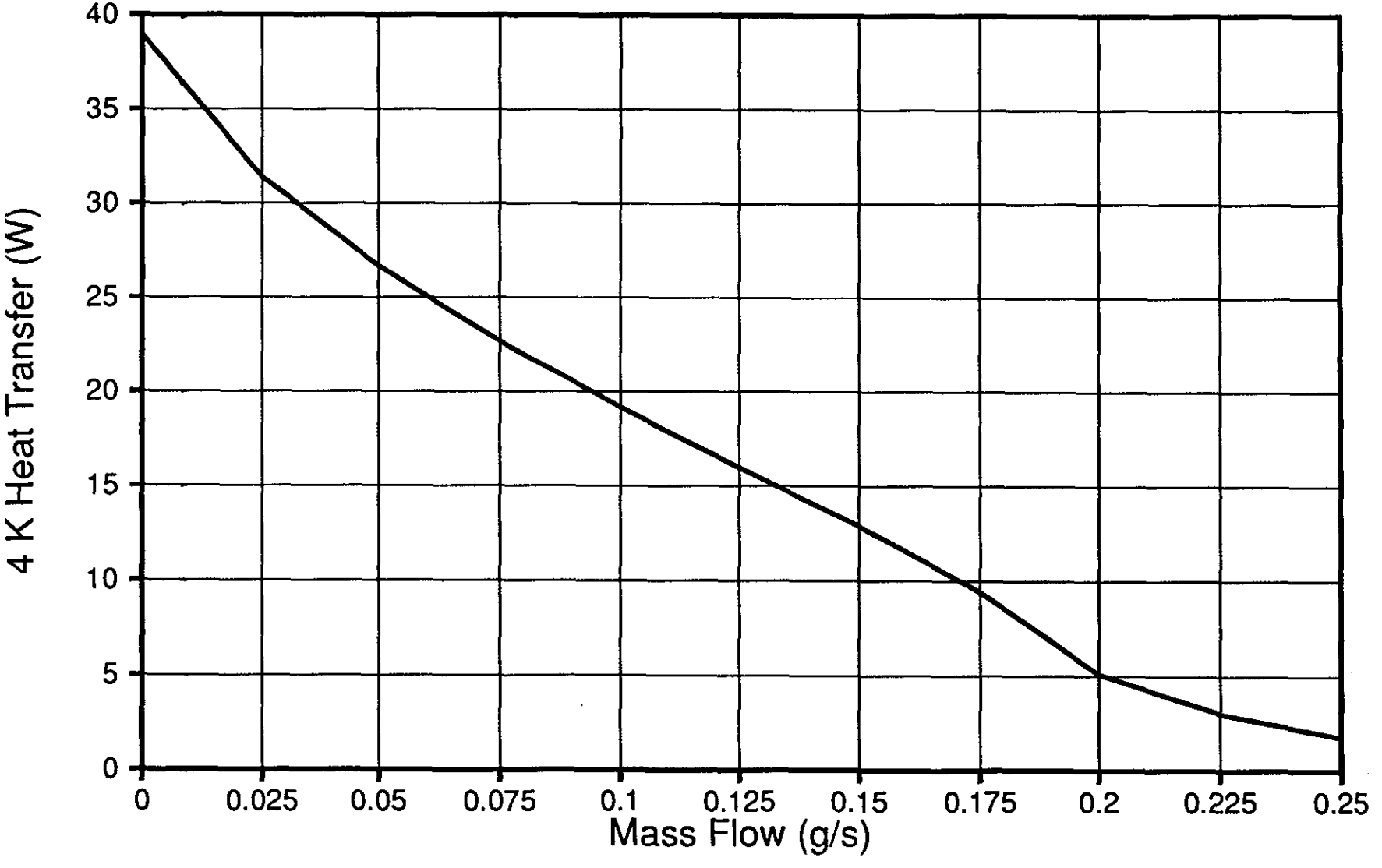

FIGURE 9: ASST LEAD CARNOT CRYO SYSTEM WORK FOR STEADY STATE AT I=0 KA

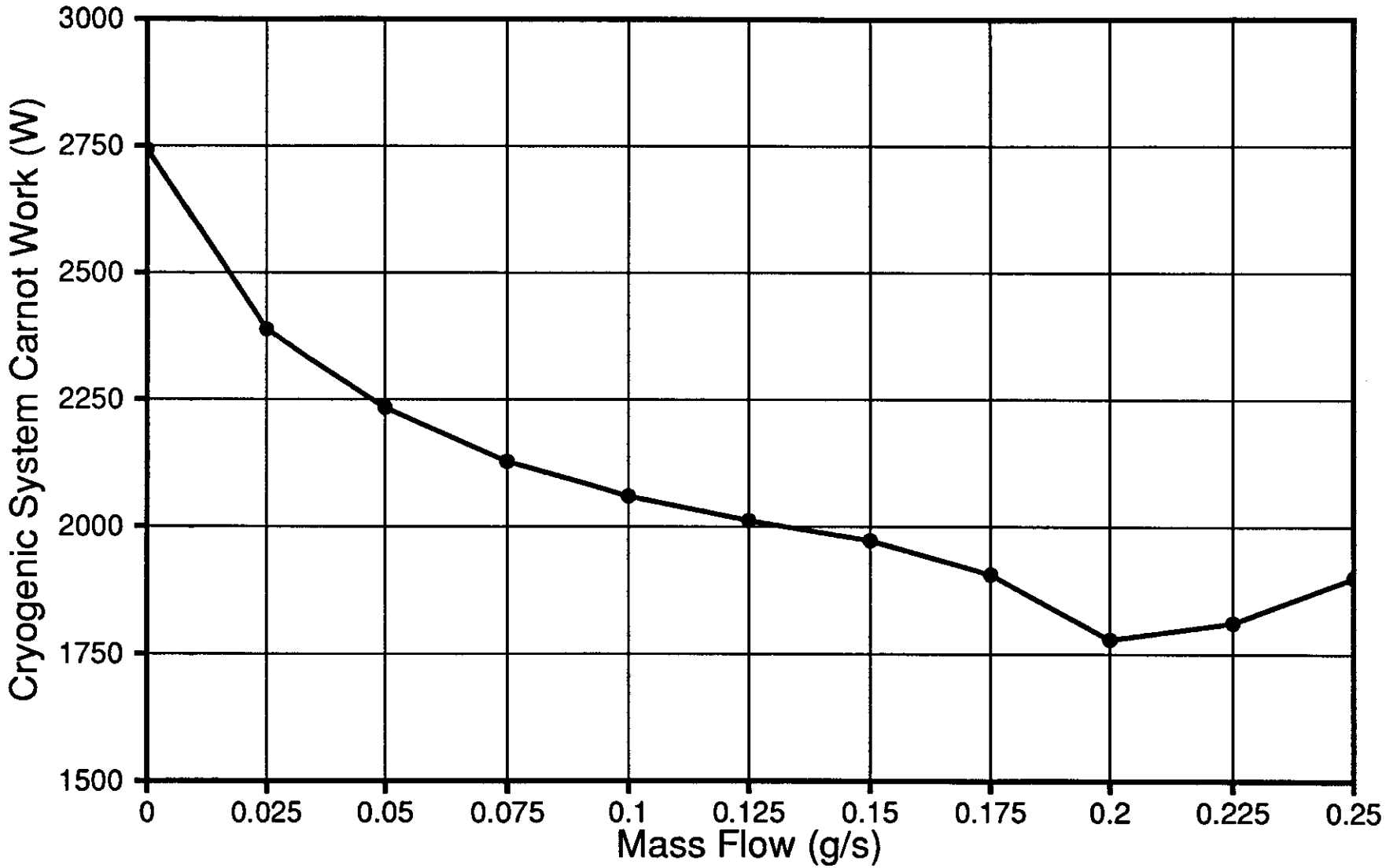

SSC/ASD/CRYO/JAD/09-15-93

FIGURE 10: ASST POWER LEAD FOR COLLIDER OPERATION
WARM END STEADY STATE TEMPERATURE PREDICTIONS

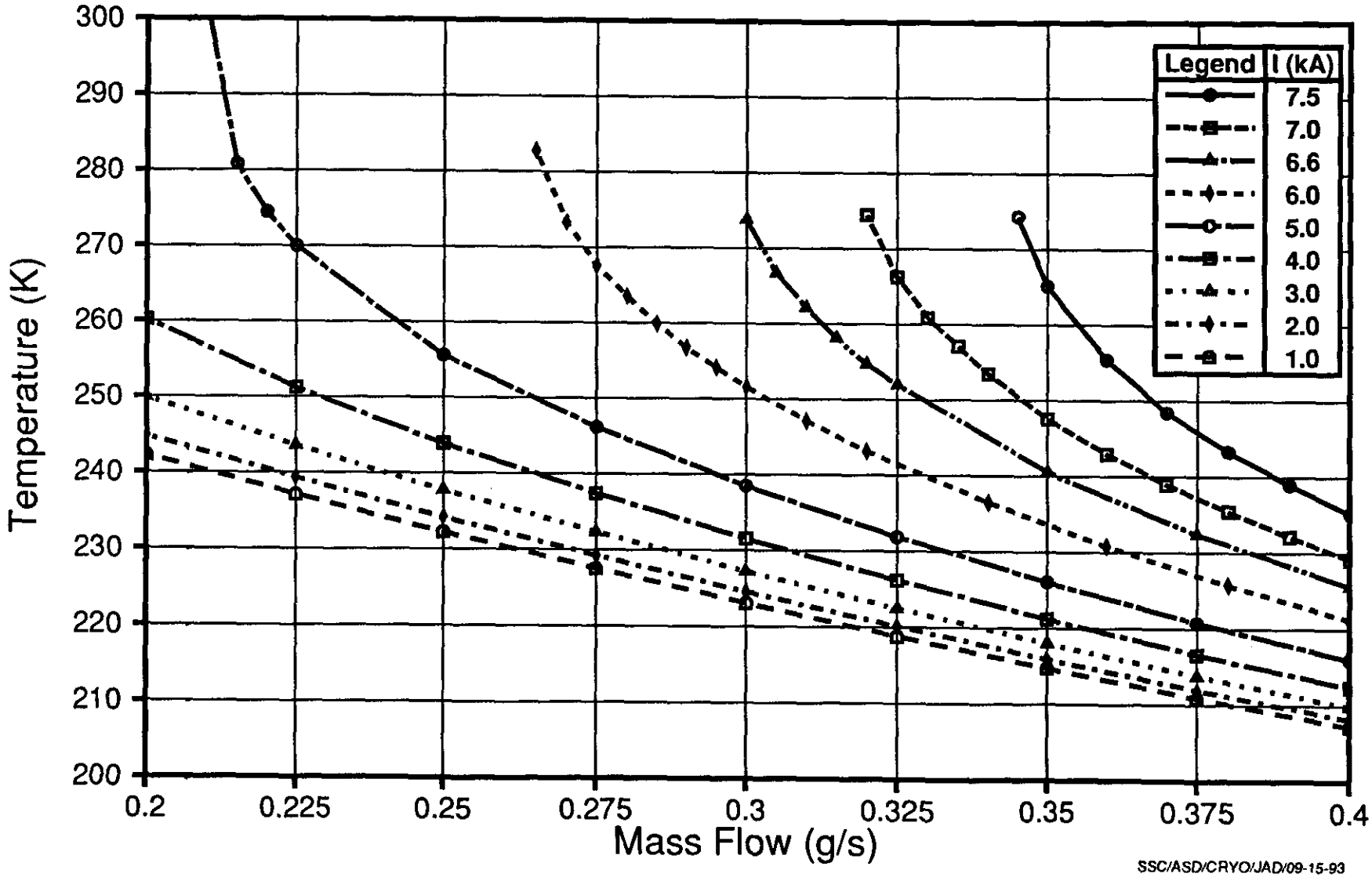

FIGURE 11: ASST POWER LEAD FOR COLLIDER OPERATION
COLD END STEADY STATE TEMPERATURE PREDICTIONS

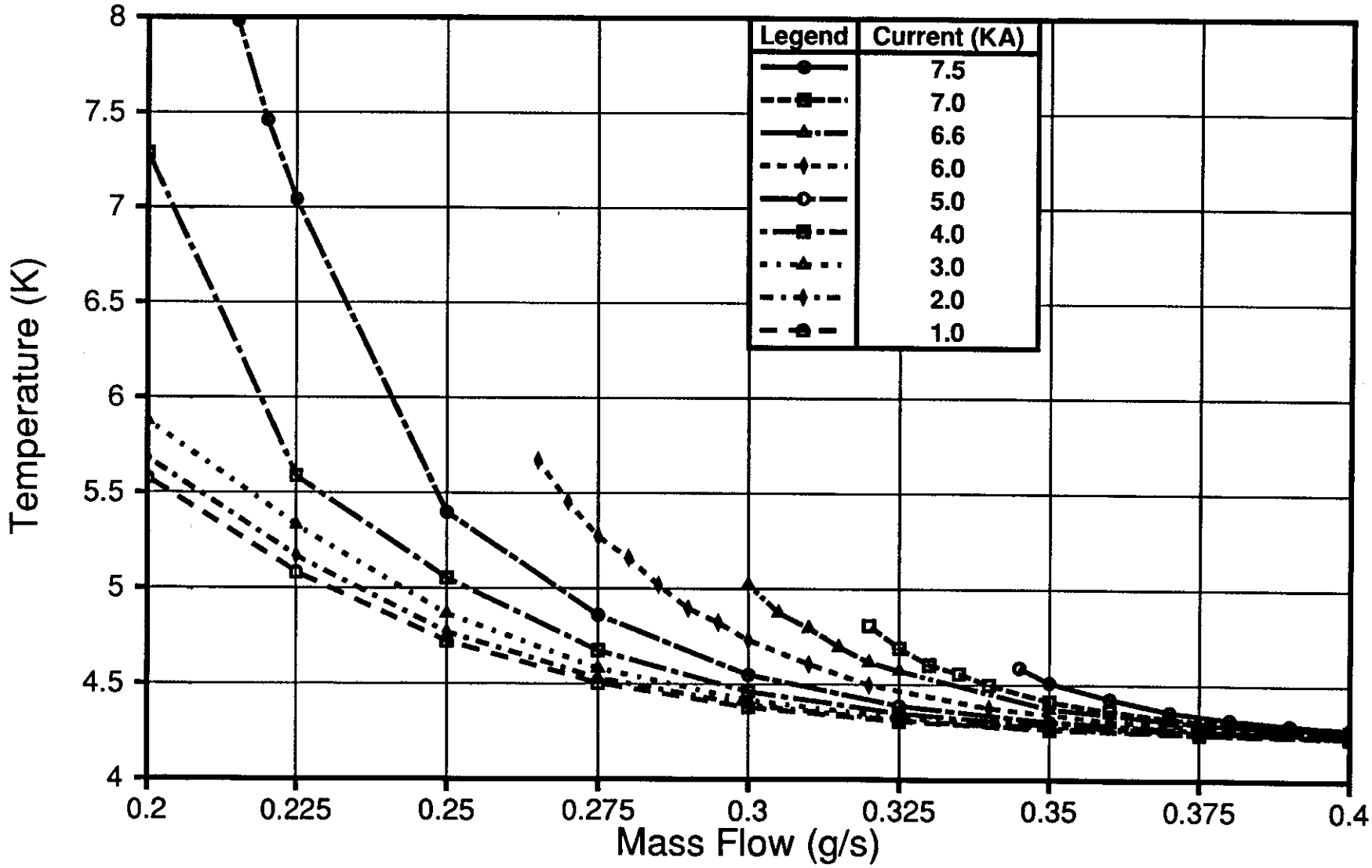

SSC/ASD/CRYO/JAD/09-20-93

FIGURE 12: ASST POWER LEAD FOR COLLIDER OPERATION
COLD END STEADY STATE HEAT TRANSFER

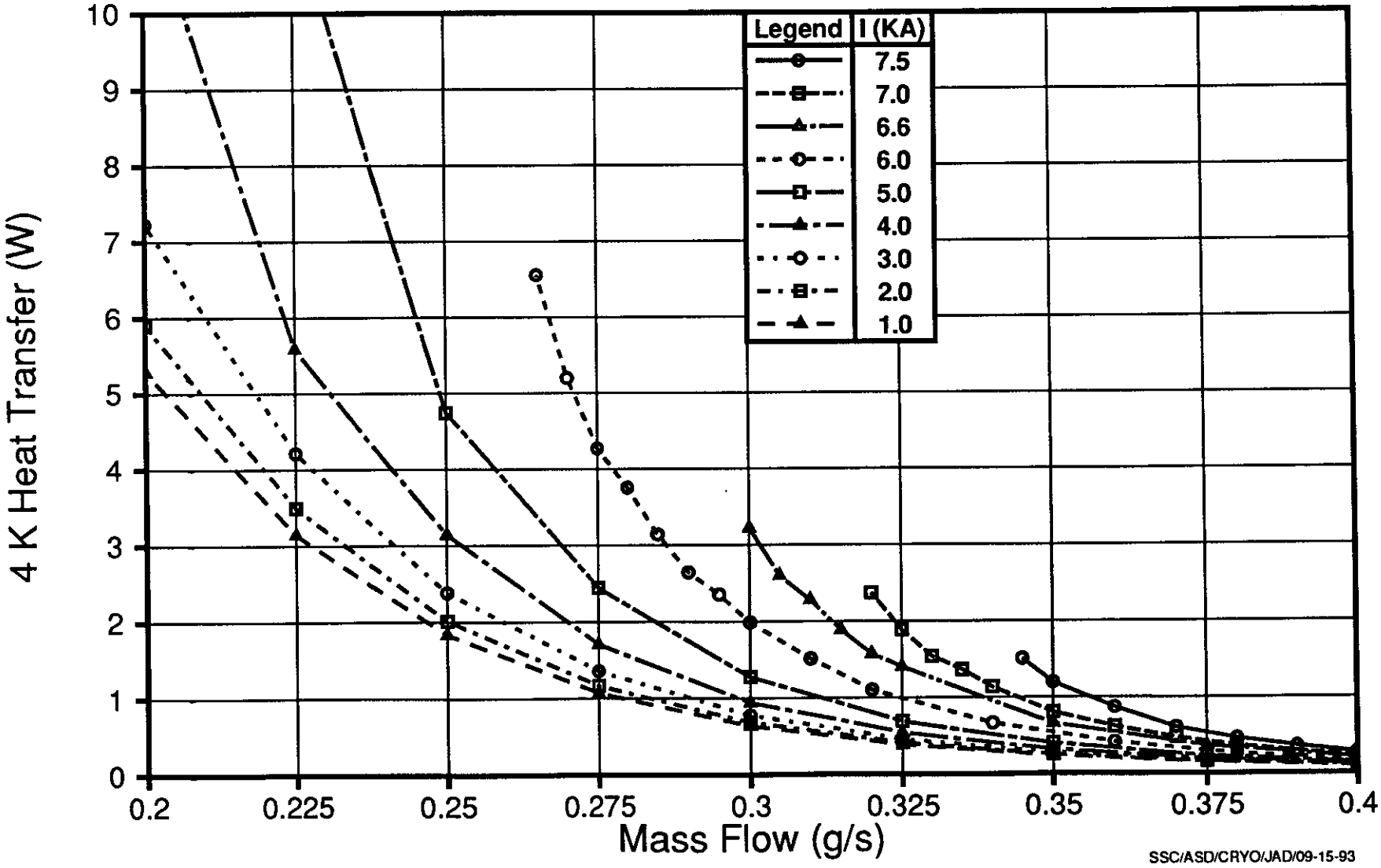

FIGURE 13: ASST POWER LEAD FOR COLLIDER OPERATION
PREDICTED CRYOGENIC SYSTEM CARNOT WORK

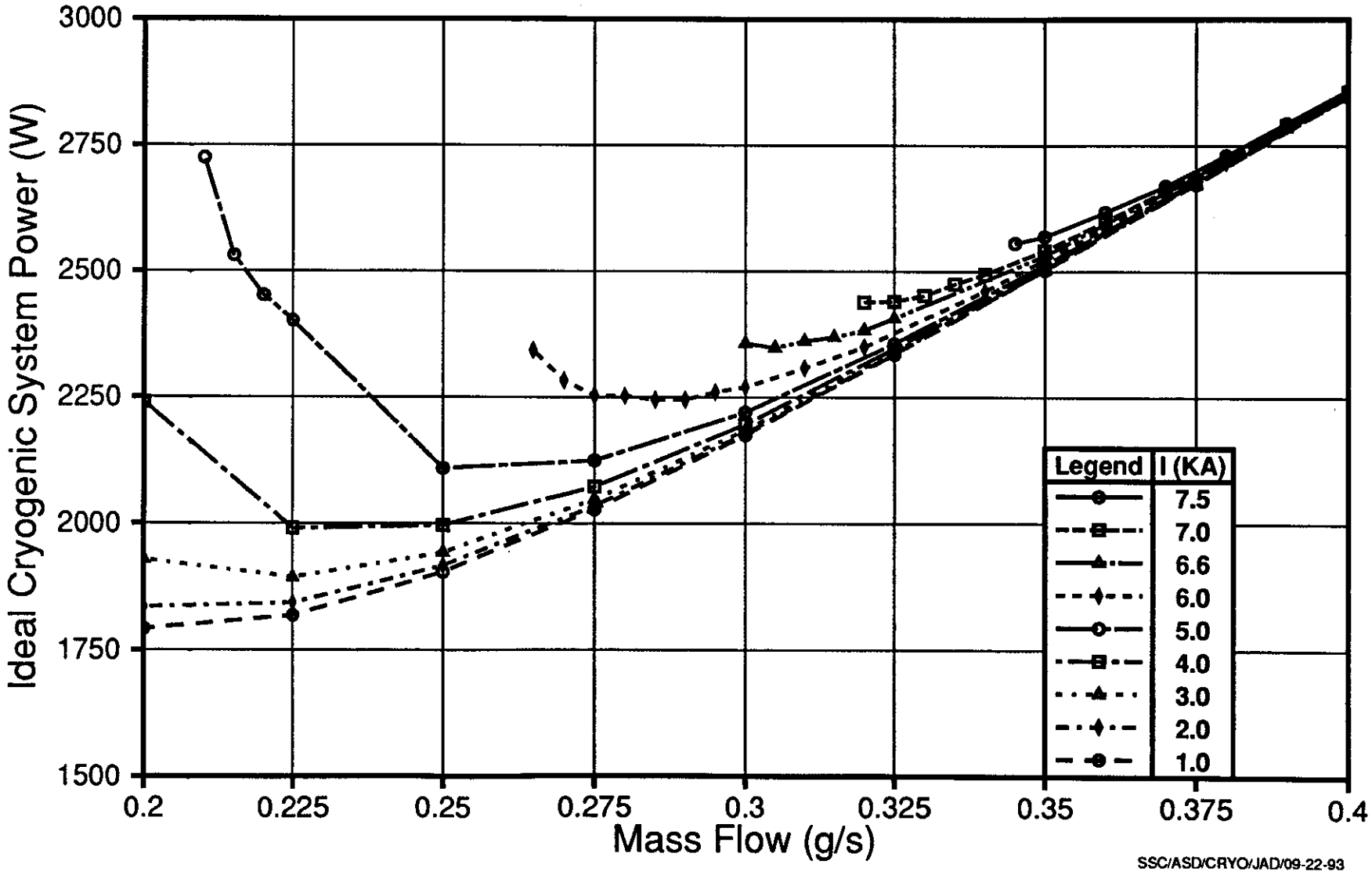

FIGURE 14: ASST POWER LEAD FOR COLLIDER OPERATION
STEADY STATE LEAD VOLTAGE PREDICTIONS

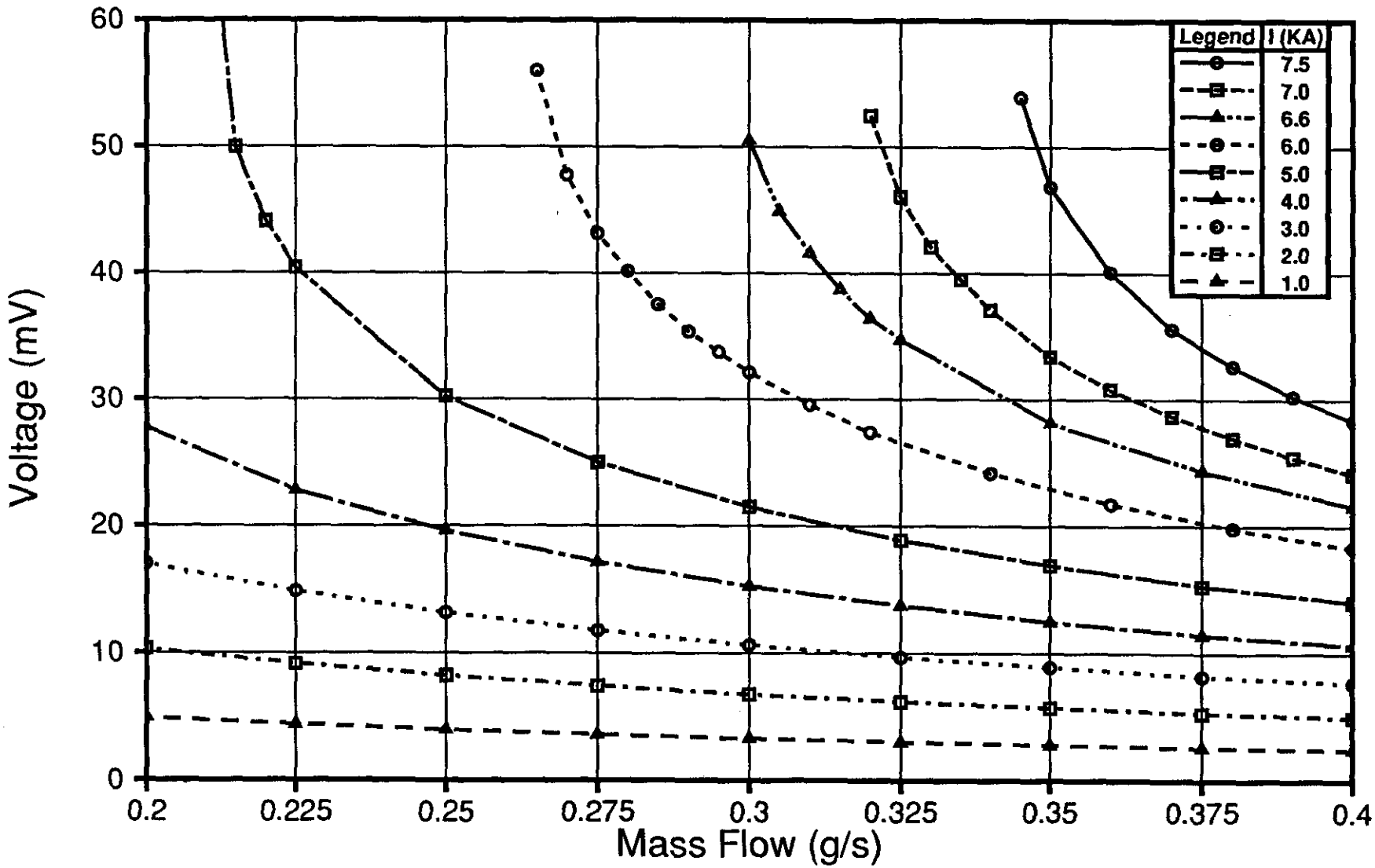

SSC/ASD/CRYO/JAD/29-SEP-93